

STABILIZATION UNDER ROUND ROBIN SCHEDULING OF CONTROL INPUTS IN NONLINEAR SYSTEMS

CHINMAY MAHESHWARI

*Department of Mechanical Engineering
IIT Bombay, Powai
Mumbai 400076, India*

SUKUMAR SRIKANT AND DEBASISH CHATTERJEE

*Systems and Control Engineering
IIT Bombay, Powai
Mumbai 400076, India
<http://www.sc.iitb.ac.in/~srikant>
<http://www.sc.iitb.ac.in/~chatterjee>*

ABSTRACT. We study the qualitative behavior of multivariable control-affine nonlinear systems under sparsification of feedback controllers. Sparsification in our context refers to the scheduling of the individual control inputs one at a time in rapid periodic sweeps over the set of control inputs, which we call the round robin scheduling. We prove that if a locally asymptotically stabilizing feedback controller is sparsified via the round robin scheme and each control action is scaled appropriately, then the corresponding equilibrium of the resulting system is stabilized when the scheduling is sufficiently fast; under mild additional conditions, local asymptotic stabilization of the corresponding equilibrium can also be guaranteed. Our technical tools are derived from optimal control theory, and our results also contribute to the literature on the stability of switched systems in the fast switching regime. Illustrative numerical examples depicting several subtle features of our results are included.

§1. INTRODUCTION

For positive integers d and m , consider a control-affine nonlinear system with m control inputs

$$(1.1) \quad \dot{x}(t) = f(x(t)) + \sum_{i=1}^m g_i(x(t))u_i(t),$$

E-mail addresses: {chinmay_maheshwari, srikant.sukumar, dchatter}@iitb.ac.in.

Key words and phrases. nonlinear control, stabilization, switched systems, sparsity, scheduling.

where $f : \mathbb{R}^d \rightarrow \mathbb{R}^d$ is a smooth drift vector field, $g_i : \mathbb{R}^d \rightarrow \mathbb{R}^d$ are smooth control vector fields for each i , and $x(t) \in \mathbb{R}^d$ is the vector of states and $u_i(t) \in \mathbb{R}$ is the i^{th} control action at time t . Since the beginning of control theory, the underlying assumption has been that all the m control inputs are at the disposal of the control designer at every instant of time. The exercise of scheduling of controllers and sensors in a way such that not all of them are active at every instant, is slowly gaining momentum, driven by concrete applications in the broad area of networked control systems ([WY01, GIL07]). In large scale networked control systems, typically, the actuation and sensing capabilities are resources that are shared between various sub-systems, and therein such scheduling is motivated by the need to reduce cost and complexity. In addition, simultaneously commanding m control inputs at every instant of time, especially when working with high-dimensional systems ($d, m \gg 1$), is becoming a challenging task [CPRT17, p. 111] today, especially since such systems routinely arise in the context of multi-agent systems [CPRT17], traffic networks [CC10], smart grids [CM12, CHW11], etc.

A common feature in such systems is the fact that the active engagement of all the control inputs simultaneously leads to undesirable consequences such as increased communication costs, higher maintenance requirements, wireless signal interference, lack of flexibility, etc. Naturally, on the one hand, a reduction in the number of control inputs that are simultaneously active at every time instant, is a desirable feature. On the other hand, reducing the active control inputs without proper care may be disastrous, leading to loss of key system-theoretic properties such as controllability. Indeed, the finding the fewest actuators for linear systems while retaining controllability of the system is a hard problem from a computational complexity standpoint; see [PKS13] and the references therein.

In this article we take advantage of sparsity to reduce the number of control actions that are simultaneously active. We think of each (scalar) control variable in a multidimensional controller as a separate entity, and sparsify the application of the control actions by

- switching, at each time instant, only one of the inputs to the ‘on’ or active state, while the rest are forced to attain the zero value (their ‘off’ or inactive states), and
- cycling rapidly over the set of inputs in a round robin fashion.

The article at hand studies the effect of the preceding scheduling scheme in the context of stabilization of the nonlinear system (1.1).

To this end, first, we design an asymptotically stabilizing controller for (1.1) without paying attention to sparsification. This controller, synthesized under the assumption that all the control inputs are always active, is our *nominal controller*. The particular problem of synthesizing asymptotically stabilizing feedbacks for control-affine nonlinear systems is extremely well studied in the literature, and in this article we do *not* revisit this topic. Instead, we assume that such controllers are available at hand, and as and when required, we may pick a nominal controller off the shelf. Next, we apply the control actions dictated by the nominal controller via the following scheme:

- (I) we scale all the control values of the nominal controller by m (recall that m is the number of controllers), and
- (II) we pick a small number $\tau > 0$, pick an arbitrary order of the m controllers (relabel them to be $(1, 2, \dots, m)$ without loss of generality), and switch periodically every τ units of time to one of the (scaled) controllers to ‘on’ and the rest to ‘off’ during the corresponding interval of length τ .

The resulting periodic multiplexing of the control actions leads to a particular kind of on-off behavior of a part of the closed-loop vector field, thereby producing a switched dynamical system in which τ^{-1} plays the role of the *switching frequency*. In the preceding setting, we shall establish that if the switching frequency is held fixed at a sufficiently high value (equivalently, if τ is sufficiently small), then one can guarantee stability of the resulting switched system. Moreover, if the switching is made faster with time in an appropriate way (to be made precise in §2.2.2), then, in addition, asymptotic stability of the closed-loop system can be certified. We emphasize that our results proceed from the mild assumption of asymptotic stability of the closed-loop system under the nominal controller.

The amplification aspect of our scheme discussed in (I) above is a very crucial requirement for our results. Intuitively, since only one control input is active at any given instant, the amplification factor compensates for their inactive periods by depleting sufficient energy away from the system during its active period, thereby promoting stabilizing behaviour. We shall illustrate and elaborate more on the technical aspects of this scaling in §3.

The emergence of a switched dynamical system from our scheduling scheme leads to new challenges for at least two reasons. One, it is well known that unplanned switching between systems may lead to instability [Lib03] and even chaotic behaviour [GB08]. Indeed, such undesirable situations may arise in our context if one is not careful, as will be illustrated by our numerical case studies presented in §3. Two, the fast switching regime has only been sparsely investigated in the literature, and there are practically no standard results to lift off the shelf. Our technical proofs proceed ab ovo, and our key tool is borrowed from optimal control in the form of the so-called chattering lemma [BM13, Chapter 3]; in our context, this lemma assures uniform convergence, as the switching frequency diverges to infinity, of the trajectories generated by the periodically scheduled controller to the trajectories generated by the nominally controlled system. The amplification of the control actions stated in (I) plays a crucial role in this type of convergence, and is in spirit related to the ideas in [SA11] where the authors designed a high-gain feedback controller to schedule a single actuator for 3-axis stabilization of a spacecraft.

The literature on stability under sparsification of controllers is itself sparse. Two closely related studies are [CPRT17, MSBH17]. In [MSBH17] the authors design a periodic scheduling based PID controller for SCARA robots to ensure reference tracking with bounded errors, but no formal proof for the merit of the strategy is provided, and the technique employed there is limited to linear systems. The results of [CPRT17] are more aligned with our work; they cater to nonlinear systems and provide asymptotic stability certificates for control-affine systems of the form (1.1) under round-robin periodic scheduling of Jurdjevic-Quinn controllers [JQ78]. However, the drift vector fields are required to be dissipative in [CPRT17]; as a result, the uncontrolled dynamics lose “energy” with time, which means that the system exhibits inherently stable behavior under zero control. In this article we remove such restrictions on the drift vector fields; in broad strokes, the only indispensable assumption employed here is that there are asymptotically stabilizing controllers available for our control-affine system (1.1).

Our article unfolds as follows. We set up the premise of this article in §2.1. Our main results are presented in §2.2, where we provide stability certificates under round-robin periodic scheduling of control inputs. In §3 we present two numerical case studies that illustrate our main results presented §2.2. A brief summary of the results and future research directions are provided in §4. Several technical results including, among others,

the chattering lemma and a recent version of Alekseev's bound, are catalogued in Appendix A, and Appendix B contains the proofs of our main results.

Notations. Standard notations are employed here. We denote the set of non-negative integers by \mathbb{N} and the set of positive integers by \mathbb{N}^* . For a positive integer k we define $[k] := \{1, 2, \dots, k\}$. The Lebesgue measure of a measurable set $S \subset \mathbb{R}$ is written as $|S|$. If $A \subset \mathbb{R}^n$, then its interior is denoted by $\text{int}(A)$ and the closure by $\text{cl}(A)$. For a vector $x \in \mathbb{R}^n$ we write $\|x\|$ for its Euclidean norm, and for $r > 0$ we write the *closed* Euclidean ball of radius r centered at x as $\mathcal{B}[x, r] := \{y \in \mathbb{R}^n \mid \|y - x\| \leq r\}$. For $y \in \mathbb{R}$ we employ $\lfloor y \rfloor$ to denote the greatest integer dominated by y . If $v \in \mathbb{R}^n$ is given, then $\text{diag}(v)$ denotes a matrix D of dimension $n \times n$, such that $D_{ij} = v_i \delta_{ij}$, $i \in [n]$, with δ_{ij} being the Kronecker delta.

§2. MAIN RESULTS

Let us start by setting up the basic definitions needed for our main results. In what follows, the word *measurability* will always be stated for Lebesgue measurability.

For positive integers d, p and a scalar t_0 , consider the following system

$$(2.1) \quad \dot{x}(t) = f(t, x(t); \ell(t)), \quad x(t_0) = \bar{x}, \quad t \geq t_0,$$

where $x(t) \in \mathbb{R}^d$ is the vector of states at time t , and $\ell : [t_0, +\infty[\rightarrow \mathbb{R}^p$ is a time-dependent map describing the evolution of a parameter. We permit only such maps ℓ that $[t_0, +\infty[\times \mathbb{R}^d \ni (t, x) \mapsto f(t, x; \ell(t)) \in \mathbb{R}^d$ is measurable in t and locally Lipschitz in x , and refer to such maps as *admissible*. Consequently, Carathéodory solutions of (2.1) exist [Fil88, Chapter 1]. We tacitly assume that the solution is unique and that it exists for all time, and we denote it by $[t_0, +\infty[\ni t \mapsto x(t; \ell) \in \mathbb{R}^d$ after suppressing the dependence on the initial state and the initial time for the sake of brevity. Without loss of generality we suppose that $0 \in \mathbb{R}^d$ is an equilibrium point of the above system; i.e., $f(s, 0; \ell) = 0$ for all s, ℓ .

Definition 2.1. The equilibrium point 0 of (2.1) is:

(D-a) *uniformly stable* if for every $\varepsilon > 0$ there exists a pair $(\Delta, \ell(\cdot))$, where $\Delta > 0$ and $\ell(\cdot)$ is an admissible map, both independent of t_0 and dependent only on ε , such that

$$\|\bar{x}\| \leq \Delta \implies \|x(t; \ell)\| \leq \varepsilon \quad \text{for all } t \geq t_0;$$

(D-b) *uniformly asymptotically stable* if for every $\varepsilon > 0$ there exists a pair $(\Delta, \ell(\cdot))$, where $\Delta > 0$ and $\ell(\cdot)$ is an admissible map, both independent of t_0 and dependent only on ε such that

$$\|\bar{x}\| \leq \Delta \implies \|x(t; \ell)\| \leq \varepsilon \quad \text{for all } t \geq t_0;$$

and moreover, for each $\eta > 0$ there exists $T > 0$ independent of t_0 , such that with same admissible map $\ell(\cdot)$ we have

$$\|\bar{x}\| \leq \Delta \implies \|x(t; \ell)\| \leq \eta \quad \text{for all } t \geq t_0 + T.$$

Remark 2.2. We employ slightly different versions of parametric uniform stability and uniform asymptotic stability compared to the ones predominantly found in the literature [Vid02, Chapter 5]; this is because we must consider the dependence of the solution trajectories on the admissible map $\ell(\cdot)$, which plays the role of a parameter residing in some infinite-dimensional space. A notion of parameter dependent exponential stability was introduced in [PL01, Definition 1], but that definition requires uniformity in the parameter

in addition to the initial time, whereas we do *not*. To wit, we employ the word “uniform” to denote uniformity in the time argument only.

§ 2.1. Premise. For positive integers d and m , and an initial time $t_0 \geq 0$, consider the control affine system

$$(2.2) \quad \dot{x}(t) = f(x(t)) + \sum_{k=1}^m g_k(x(t))u_k(t), \quad x(t_0) = \bar{x}, \quad t \geq t_0,$$

where

(P-i) $\mathbb{R}^d \ni \xi \mapsto f(\xi) \in \mathbb{R}^d$ and $\mathbb{R}^d \ni \xi \mapsto g_k(\xi) \in \mathbb{R}^d$ for $k \in [m]$ are continuously differentiable maps.

Let $\mathbb{R}^d \ni \xi \mapsto \phi(\xi) := (\phi_k(\xi))_{k \in [m]} \in \mathbb{R}^m$ be a m -dimensional feedback. Such feedbacks may arise from, depending on the control objective and the specific systems under consideration, the Artstein-Sontag universal formula, Jurdjevic-Quinn controllers, Lyapunov and/or dynamic programming based synthesis techniques, etc.

The application of a stabilizing feedback ϕ to (2.2) produces the closed-loop control system

$$(2.3) \quad \dot{x}(t) = f(x(t)) + \sum_{k=1}^m g_k(x(t))\phi_k(x(t)), \quad x(t_0) = \bar{x}, \quad t \geq t_0,$$

where we stipulate that:

- (P-ii) the map $\mathbb{R}^d \ni \xi \mapsto f(\xi) + \sum_{k=1}^m g_k(\xi)\phi_k(\xi) \in \mathbb{R}^d$ is continuously differentiable (for which it suffices to assume that ϕ is continuously differentiable), and
- (P-iii) the closed-loop dynamics (2.3) has an
 - isolated,
 - hyperbolic,¹ and
 - locally asymptotically stable equilibrium at 0.

As a consequence of (P-iii), $f(0) + \sum_{k=1}^m g_k(0)\phi_k(0) = 0$. We further assume that

(P-iv) $f(0) = 0$, and $\phi_k(0) = 0$ for each $k \in [m]$.

While (P-iv) is not crucial for our proofs to hold (indeed, it is sufficient to require that $f(0) + mg_k(0)\phi_k(0) = 0$ for each k), the property (P-iv) holds for a large class of standard stabilizing feedbacks including the Artstein-Sontag universal formula and the Jurdjevic-Quinn controllers to name a few, and this assumption will simplify our presentation.

As mentioned in the Introduction, the selection of the particular feedback ϕ is *not* under consideration in the article at hand; we assume that there is a sufficiently large library of feedback controllers that satisfy the properties (P-i)-(P-iv) for a given system, from which the control designer may pick one that suits them. Instead, here we are interested in the effect of scheduling the individual components of such a stabilizing feedback in a fast round robin fashion. This scheduling has been viewed in [CPRT17] as a ‘spatial’ sparsification

¹Recall that an equilibrium point of a nonlinear system with a continuously differentiable vector field is *hyperbolic* if the first order term in the Taylor’s expansion of the vector field at that equilibrium point has no purely imaginary eigenvalue.

of the control in the sense that only one of the control components is active at any given instant of time.

§2.2. Main Results. In this subsection we present the main results of this article. First, in §2.2.1 we present the case where a family of locally asymptotically stabilizing controller for (2.2) is employed in a periodic fashion with constant switching frequency. Second, in §2.2.2 we discuss the effect of monotonically increasing the switching frequency over equispaced intervals of time. We provide a certificate of uniform stability in the sense of Definition (D-a) for the closed-loop equilibrium in the former case, while in the latter case we provide a guarantee of uniform asymptotic stability in the sense of Definition (D-b).

§2.2.1. Uniform stability under constant switching frequency. Fix $\tau > 0$ and $t_0 \geq 0$. Let $[t_0, +\infty[$ be partitioned into a countable family of disjoint half-open intervals of length $m\tau$ as $[t_0, +\infty[= \bigcup_{n \in \mathbb{N}^*} [t_0 + (n-1)m\tau, t_0 + nm\tau[$. We stipulate a periodic scheduling of the feedback controllers defined in §2.1 over $[t_0, t_0 + m\tau[$ with the objective of inducing temporal sparsity in the family of the m controllers, and repeat the same scheme over successive such intervals. In other words, for each n , we partition the interval $[t_0 + nm\tau, t_0 + (n+1)m\tau[$ into m contiguous intervals of length τ each, and activate just the k^{th} controller during the k^{th} such temporal sub-interval. Accordingly, we define the following piecewise constant switching signal:

$$(2.4) \quad [0, +\infty[\ni t \mapsto \sigma(t, \tau) := 1 + \left\lfloor \frac{t - m\tau \left\lfloor \frac{t}{m\tau} \right\rfloor}{\tau} \right\rfloor \in [m]$$

that selects, at each $t \geq 0$, the index $\sigma(t, \tau)$ in the set $[m]$; we call σ the *switching scheme* with *switching time* τ .

Let us consider the following closed-loop system under the switching scheme σ with the feedback $\phi(\cdot) = (\phi_k(\cdot))_{k \in [m]}$ replaced by its scaled version $m\phi(\cdot) = (m\phi_k(\cdot))_{k \in [m]}$:

$$(2.5) \quad \dot{y}(t) = f(y(t)) + mg_{\sigma(t-t_0, \tau)}(y(t))\phi_{\sigma(t-t_0, \tau)}(y(t)), \quad y(t_0) = \bar{x}, \quad t \geq t_0.$$

In the light of (P-iv), it is readily observed that the point $0 \in \mathbb{R}^d$ is an equilibrium point of the switched system (2.5).

Remark 2.3. We have scaled each of the feedback functions $\phi_k(\cdot)$ by a factor of m in (2.5). Since the switching scheme σ permits only one ϕ_k to be active ‘on’ at a given time, this extra factor of m , roughly speaking, extracts sufficient “energy” from the system during its ‘on’ stage to compensate for the inactivity during its ‘off’ period in order to stabilize the equilibrium point.

Theorem 2.4 below, whose proof is deferred to Appendix B.1, asserts that under the round-robin periodic scheduling with constant switching frequency, the equilibrium point $0 \in \mathbb{R}^d$ of the closed-loop system (2.5) is uniformly stable in the sense of Definition (D-a).

Theorem 2.4. *Consider the control system (2.2) along with its associated data (P-i). Suppose that we pick a feedback $\phi(\cdot)$ such that the closed-loop system (2.3) satisfies (P-ii)-(P-iv). Then the equilibrium $0 \in \mathbb{R}^d$ of (2.5) is uniformly stable in the sense of Definition (D-a).*

Moreover, for every $\varepsilon > 0$, there exist $\Delta, \bar{\tau} > 0$, both independent of t_0 , such that for all $\tau \in]0, \bar{\tau}]$ and with the switching signal $\sigma(\cdot, \tau)$ defined in (2.4), the solution of (2.5) satisfies

$$\|\bar{x}\| \leq \Delta \implies \|y(t)\| \leq \varepsilon \quad \text{for all } t \geq t_0.$$

This theorem caters to the ‘fast switching’ regime in the switched systems literature, an area where there have been far fewer investigations compared to the more well-known ‘slow switching’ regime treated extensively in the standard textbook [Lib03, Chapters 3, 4] and more recently surveyed in [KC17]. Intuition suggests that Theorem 2.4 pertains to a type of averaging on a fast time-scale. Indeed, the chattering lemma, popularly employed for various types of convexification in the context of optimal control theory, is the key tool needed in our proofs. This state of affairs points to the possibility of employing, more generally, Young measures in the context of averaging along the lines of [Art08], which is currently under investigation and will be reported in subsequent articles.

§2.2.2. Uniform asymptotic stability under increasing switching frequencies. Theorem 2.4 dealt with uniform stability of the round-robin periodically scheduled (switched) system (2.5) under a constant switching frequency. However, in control engineering we are often interested in ensuring asymptotic convergence of system trajectories to the equilibrium point. It turns out (as we shall assert in Theorem 2.5), that increasing the switching frequency periodically so that the frequency becomes unbounded asymptotically in time guarantees uniform asymptotic stability of the equilibrium point of the resulting switched system.

Fix $t_0 \geq 0$ and $T > 0$. Let $[0, +\infty[\ni t \mapsto \tilde{\tau}(t) \in]0, +\infty[$ be a piecewise constant non-increasing function satisfying $\tilde{\tau}(t) \xrightarrow[t \rightarrow +\infty]{} 0$. If $\tau' : [0, +\infty[\rightarrow \mathbb{R}$ is another piecewise constant non-increasing function satisfying $\tau'(t) \xrightarrow[t \rightarrow +\infty]{} 0$, we say that $\tilde{\tau}$ *dominates* τ' if $\tilde{\tau}(t) \leq \tau'(t)$ for each t .² We define a new (time-varying) switching signal dependent on $\tilde{\tau}$

$$(2.6) \quad [0, +\infty[\ni t \mapsto \tilde{\sigma}(t; \tilde{\tau}) := 1 + \left\lfloor \frac{t - m\tilde{\tau}(t) \left\lfloor \frac{t}{m\tilde{\tau}(t)} \right\rfloor}{\tilde{\tau}(t)} \right\rfloor \in [m].$$

The interval $[t_0, +\infty[$ is partitioned, depending on $\tilde{\tau}(\cdot)$, into a countable family of disjoint half-open intervals of length T as $[t_0, +\infty[= \bigcup_{n \in \mathbb{N}^*} J_n$, where $J_n := [t_0 + (n-1)T, t_0 + nT[$; by definition, on each interval J_n the function $\tilde{\tau}(\cdot)$ is held constant.

Here we are interested in establishing the asymptotic convergence of the following closed-loop system derived from (2.3) under the switching signal $\tilde{\sigma}$ with the feedback $\phi(\cdot) = (\phi_k(\cdot))_{k \in [m]}$ replaced by its scaled version $m\phi(\cdot) = (m\phi_k(\cdot))_{k \in [m]}$:

$$(2.7) \quad \dot{z}(t) = f(z(t)) + m g_{\tilde{\sigma}(t-t_0; \tilde{\tau})}(z(t)) \phi_{\tilde{\sigma}(t-t_0; \tilde{\tau})}(z(t)), \quad z(t_0) = \bar{x}, \quad t \geq t_0,$$

where \bar{x} is the same initial vector as in (2.3).

Against the preceding backdrop, we present the following theorem whose proof is deferred to Appendix B.2. It guarantees the existence of a piecewise constant non-increasing function $\tilde{\tau}$ that encodes the switching time information, such that the equilibrium for the closed-loop system (2.7) is locally uniformly asymptotically stable.

Theorem 2.5. *Consider the control system (2.2) along with its associated data (P-i). Suppose that we pick a feedback $\phi(\cdot)$ such that the closed-loop system (2.3) satisfies (P-ii)-(P-iv). Then the equilibrium of $0 \in \mathbb{R}^d$ of (2.7) is locally uniformly asymptotically stable in the sense of Definition (D-b).*

²The word *domination* here sounds more appropriate when we note that the ‘frequency’ of $\tilde{\tau}$ compared to τ' is indeed higher.

Moreover, for every $\varepsilon > 0$, there exists a pair $(\Delta, \tau'(\cdot))$, independent of t_0 , where $\Delta > 0$ and $[t_0, +\infty[\ni t \mapsto \tau'(t) \in]0, +\infty[$ is a piecewise constant non-increasing map, such that

- for every $\tilde{\tau}$ that dominates τ' , with the switching signal $\tilde{\sigma}(\cdot; \tilde{\tau})$ defined in (2.6), we have

$$\|\bar{x}\| \leq \Delta \implies \|z(t)\| \leq \varepsilon \quad \text{for all } t \geq t_0,$$

and

- for every $\eta > 0$, there exists $\tilde{T} > 0$, independent of t_0 , such that with the same switching signal $\tilde{\sigma}(\cdot; \tilde{\tau})$, we have

$$\|\bar{x}\| \leq \Delta \implies \|z(t)\| \leq \eta \quad \text{for all } t \geq t_0 + \tilde{T}.$$

Remark 2.6. The underlying premise of the preceding discussion is that at any instant of time only *one* out of m feedbacks is permitted to stay ‘on’. However, our analysis carries over to the situation when there is an ensemble of control-affine nonlinear systems, and each control input u_i is itself a multi-variable control catering to its own stand-alone system; we construct the aggregate high-dimensional control system by stacking the individual systems in a natural way, thereby distilling the aggregated high-dimensional drift and control vector fields. Although there is no a priori coupling between the individual systems at the stage of this definition, a nominal (feedback) controller for this aggregated system may well introduce such coupling terms via the resulting feedbacks. An identical analysis as ours may be carried hereafter by scheduling the family of inputs (u_i) as discussed above.

§3. NUMERICAL EXPERIMENTS

In this section we present comprehensive numerical studies of two control systems, namely, a coupled inverted pendulum on a cart and a mass-spring system; and a spacecraft attitude control system when the control inputs are scheduled in a periodic fashion as discussed above. In the former example, we employ a constant switching rate based scheduling (discussed in §2.2.1) while in the latter we use time-varying scheduling with the switching rate monotonically increasing and diverging with time (discussed in §2.2.2).

§3.1. Linearized model of an inverted pendulum on a cart coupled with a mass-spring system. We start with a contrived example derived from the (Taylor’s) linearization of an inverted pendulum on a cart about its upright unstable equilibrium point and a mass-spring system. This example illustrates several features of Theorem 2.4, including the fact that for a fixed stabilizing feedback,

- it is possible to ensure uniform stability under fast round robin switching,
- slow switching may lead to instability, and
- omitting the scaling of the control actions by m may lead to instability when the corresponding scaled control actions gives uniform stability.

Quantity	Values
Time of simulation	50 s
Switching time	0.5 s
ODE solver	4-th order RK
Step length	0.05 s
Mass of the cart	3 kg
Mass of the pendulum	0.25 kg
Acceleration due to gravity	9.81 kgms ⁻²
Initial condition	$(0, \frac{\pi}{10}, 0, 0, 1, 1.05)^\top$

TABLE 1. Numerical parameters used in (3.1).

The control system at hand can be represented as follows:

$$(3.1) \quad \dot{x}(t) = \underbrace{\begin{pmatrix} 0 & 1 & 0 & 0 & 0 & 0 \\ 0 & 0 & \frac{-mg}{M} & 0 & 0 & 0 \\ 0 & 0 & 0 & 1 & 0 & 0 \\ 0 & 0 & \frac{(m+M)g}{LM} & 0 & 0 & 0 \\ 0 & 0 & 0 & 0 & 0 & 1 \\ 0 & 0 & 0 & 0 & -1 & 0 \end{pmatrix}}_{=:A} x(t) + \underbrace{\begin{pmatrix} 0 & 0 \\ \frac{1}{M} & 0.1 \\ 0 & 0 \\ \frac{-1}{LM} & 0.1 \\ 0 & 0 \\ 0.1 & 1 \end{pmatrix}}_{=:B} \begin{pmatrix} u_1(t) \\ u_2(t) \end{pmatrix},$$

where $x := (x_{IP}, x_{MS}) \in \mathbb{R}^6$, with $x_{IP} \in \mathbb{R}^4$ denoting the states of the inverted pendulum on a cart, and $x_{MS} \in \mathbb{R}^2$ representing the states of the mass-spring system. In (3.1) the quantity M denotes the mass of the cart, m denotes the mass of the pendulum, L is the length of the pendulum, and g refers to the acceleration due to gravity.

The drift vector field in (3.1) corresponding to the inverted pendulum is unstable due to the fact that the upright vertical position of the inverted pendulum is unstable. The two systems are coupled via the matrix B in (3.1), and this coupling has been artificially introduced for illustrative purposes only and is not motivated by physical considerations. Due to this coupling, the control input that corresponds ideally to the mass-spring system may contribute to a detrimental behaviour of the pendulum during its ‘on’ periods, and conversely.

Recall that if there exists a matrix K such that the matrix $(A - BK)$ is Hurwitz then the feedback controller $u = -Kx$ when applied to (3.1) makes the corresponding closed-loop system globally exponentially stable at the origin (hence it is asymptotically stable as well). We pick any such gain K , and employ this feedback via the switching scheme (2.4) to arrive at the analogue of (2.5) for the present example. The data employed in our experiments is presented in Table 1.

As per our discussion in the preceding sections, in the periodic scheduling we keep all but one feedbacks in the ‘off’ mode (see Fig. 3). The plant in the current control system has at least one unstable direction due to the unstable behavior of the pendulum about its upright vertical state; this leads to the divergence of the trajectories during the off-phase of the control actuation for the corresponding states. Some of the system trajectories in Fig. 1 and Fig. 2 exhibit fluctuations precisely due to this feature.

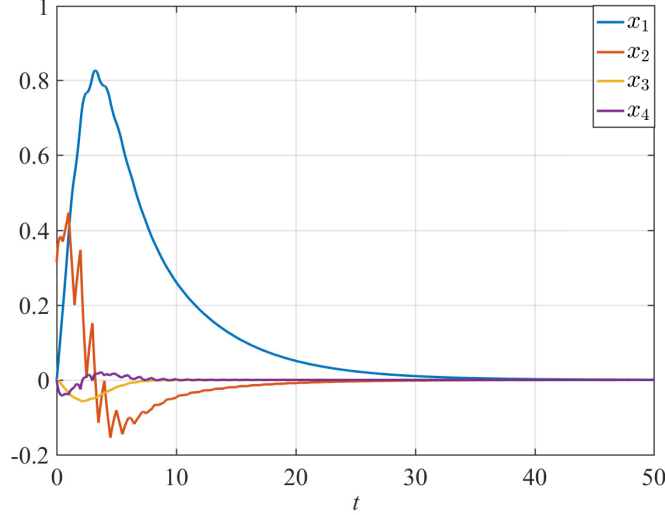


FIGURE 1. The time evolution of the states of the inverted pendulum on a cart.

Apart from the fast round robin scheduling, the role of the amplification of the control action (discussed in Remark 2.3) proves to be important for uniform stability. Indeed, if we remove this amplification factor, then the system trajectories may, in fact, diverge, as illustrated in Fig. 4.

Theorem 2.4 asserts that the equilibrium point of the system under fast periodic scheduling of its controllers is uniformly stable. However, it is interesting to note that the trajectories in this particular example appear to be exponentially stable (see Fig. 5). A formal proof of the same is not available at this juncture.

§3.2. Attitude control of spacecraft. Spacecraft are typically laden with instruments such as antennas, solar panels, etc., which must be pointed in specific directions in space for optimal performance of these instruments. The attitude (orientation) control of spacecraft is, therefore, of paramount importance today; more details on this control problem may be found in [WD91]. In this section we deploy an asymptotically stabilizing controller for spacecraft attitude in the round robin fashion with time-varying switching rates. This example illustrates several features of our main results, including

- asymptotic stability under monotonically diverging switching rates,
- the effect of not amplifying the nominal controller before application, and
- instability under slow (but constant) scheduling.

The attitude dynamics of a rigid spacecraft are modeled by Euler's equations along with a suitable representation of the attitude [LA05]. The attitude dynamics relate the angular velocity of the spacecraft in the body frame to the net external torque acting on the spacecraft, and Euler's equations are derived from the rotational dynamics via Newton's laws. The attitude kinematics, with quaternions representing the attitude, and Euler's

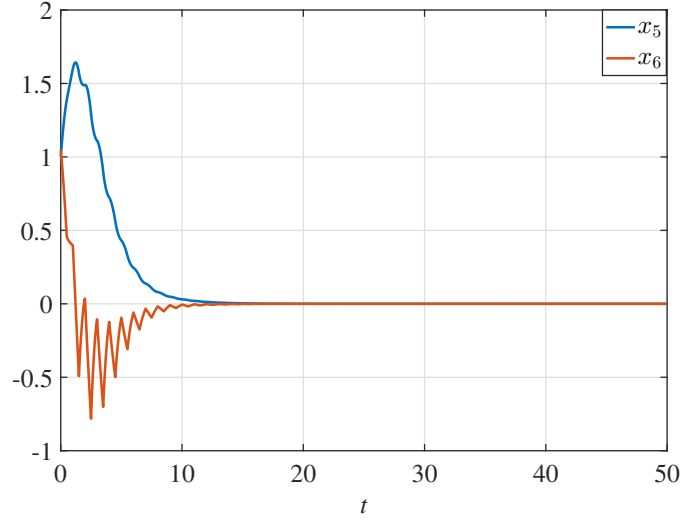


FIGURE 2. The time evolution of the states of the mass-spring system.

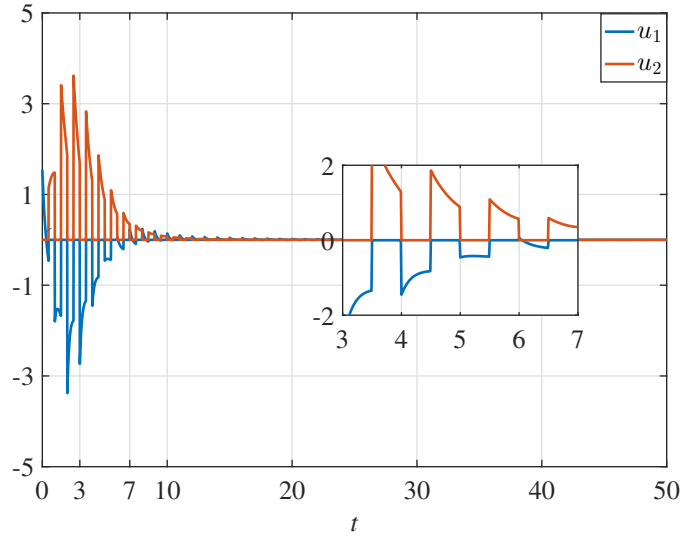


FIGURE 3. Control trajectories for the inverted pendulum (in blue) and the mass-spring system (in red)

equations together are given by

$$\begin{aligned}
 \dot{q}_0(t) &= -\frac{1}{2}q_v^\top(t)\omega(t) \\
 \dot{q}_v(t) &= \frac{1}{2}(q_0(t)\omega(t) + q_v(t) \times \omega(t)) \\
 I\dot{\omega}(t) &= -\omega(t) \times I\omega(t) + \mathcal{T}(t),
 \end{aligned}
 \tag{3.2}$$

where $\omega(t) \in \mathbb{R}^3$ is the spacecraft angular velocity expressed in body frame at time t , $I \in \mathbb{R}^{3 \times 3}$ is the (constant) inertia matrix of the rigid body, $\mathcal{T}(t)$ is the external torque

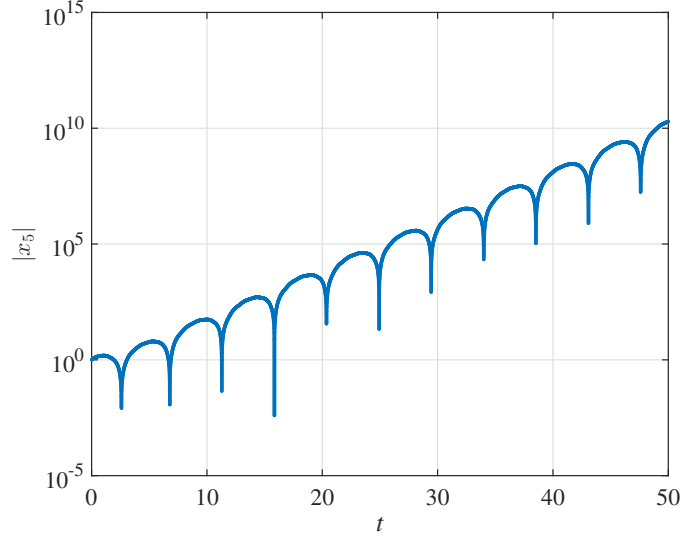


FIGURE 4. Time evolution of $|x_5(\cdot)|$ in (3.1) when the multiplicative factor of m is omitted.

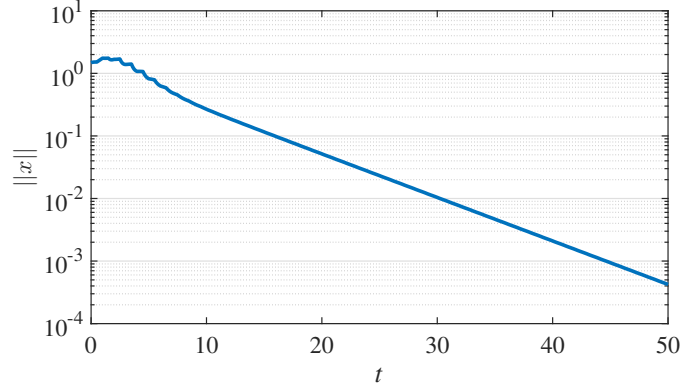


FIGURE 5. Time evolution of $\|x(\cdot)\|$ on a log scale for (3.1).

acting on the spacecraft at time t , and the pair $(q_0(t), q_v(t)) \in \mathbb{R} \times \mathbb{R}^3$ constitutes the unit quaternion at time t , i.e., $q_0^2(t) + q_v^\top(t)q_v(t) = 1$. Here the symbol \times stands for the standard cross product of vectors in \mathbb{R}^3 . The external torque \mathcal{T} in (3.2) is the feedback control acting on the rigid spacecraft that we design for attitude stabilization. For the attitude stabilization problem the equilibrium point of interest is $x_e := (\bar{q}, 0, 0, 0)$ with $\bar{q} = (1 \ 0 \ 0 \ 0)$. In an obvious way we shift the coordinate system appropriate such that $0 \in \mathbb{R}^7$ becomes the closed-loop equilibrium in order to conform with our results.

In [WD91] the authors propose an asymptotically stabilizing controller for the spacecraft attitude stabilization problem under the assumption that all control inputs are active and full state information is available at each time; we lift this feedback, given by,

$$(3.3) \quad \mathcal{T}(t) = -k_1 q_v(t) - k_2 \omega(t) \quad \text{for } t \geq 0,$$

for suitable $k_1, k_2 > 0$, and employ it as our nominal controller. Of course, $\mathcal{T}(t) \in \mathbb{R}^3$ at each t . We employ the feedback (3.3) in a periodic fashion with monotonically diverging switching frequency, and carry out simulations with the numerical values of different parameters presented in Table 2.

Quantity	Values
Time of simulation	200 s
Inertia of spacecraft	$\text{diag}((100, 70, 150)) \text{ kgm}^2$
k_1	0.5
k_2	0.1
ODE solver	4-th order RK
Step length	0.1 s
Initial value of the quaternion	$(1, 0, 0, 0)^\top$
Initial value of the angular velocities	$(0.01, 0.05, 0.03) \text{ rad s}^{-1}$

TABLE 2. Parameters used to solve for the control system (3.2) with the controller presented in (3.3).

We monotonically decrease the switching time by a factor of 0.1 starting from 0.1s in intervals of 5s. Any function that is positive, non-increasing and bounded below by the switching signal presented above would serve the purpose. Asymptotic stability of the equilibrium is guaranteed by Theorem 2.5, and is evident from Fig. 6 and Fig. 7. The prominent fluctuations in the trajectories of the system discussed in §3.1 are not so pronounced here (cf. Fig. 7) due in part to the (time varying) switching time being smaller than the one used in §3.1.

In the example presented in §3.1 the removal of the amplification factor of m (the number of control inputs) cause the trajectories to blow up as discussed in §3.1 and illustrated in Fig. 4. However, in the present system the effect is not so severe, but leads to a performance deterioration measured, e.g., in terms of settling time, as seen in Fig. 9.

If the switching frequency is not sufficiently large, then the equilibrium x_e can become unstable, and the mechanism by which this happens is fairly subtle. It is well known [Vid02, Chapter 5] that for an unforced rigid body system for which the intermediate axis is oriented in, say the x direction, any equilibrium of the form $(\bar{\omega}, 0, 0)$ with $\bar{\omega} \neq 0$ is *unstable*. For $\bar{\omega} = 1$, we tune the controller (3.3) so that the closed-loop system has an asymptotically stable equilibrium at $x_e := (\bar{q}, \bar{\omega}, 0, 0)$, which is shifted to $0 \in \mathbb{R}^7$ by employing an appropriate shift of the coordinates. Then we periodically schedule the control inputs (3.3) in a round robin fashion with a constant switching time of 18s. The results are shown in Fig. 10. In this experiment we pick one point each from $\mathcal{K}_1 := \{\bar{q}\} \times \mathcal{B}[x_e, 10^{-1}]$, $\mathcal{K}_2 := \{\bar{q}\} \times \mathcal{B}[x_e, 10^{-3}]$ and $\mathcal{K}_3 := \{\bar{q}\} \times \mathcal{B}[x_e, 10^{-5}]$ uniformly randomly to avoid any bias. Using these randomly selected points as initial conditions for the closed-loop system, we generate the trajectories in Fig. 10, where for each \mathcal{K}_i , $i \in \{1, 2, 3\}$, we label the corresponding angular velocity trajectory by $\omega_0^{(i)}$. Observe that *all* the corresponding trajectories digress away from the ball of radius 0.1 around the equilibrium. This experiment, while not a conclusive test of instability of the equilibrium, points to the fact that the aforementioned (fixed) ball around the equilibrium is being transgressed by the trajectories starting inside balls of progressively smaller (by several orders of magnitude) sizes, hinting strongly at instability

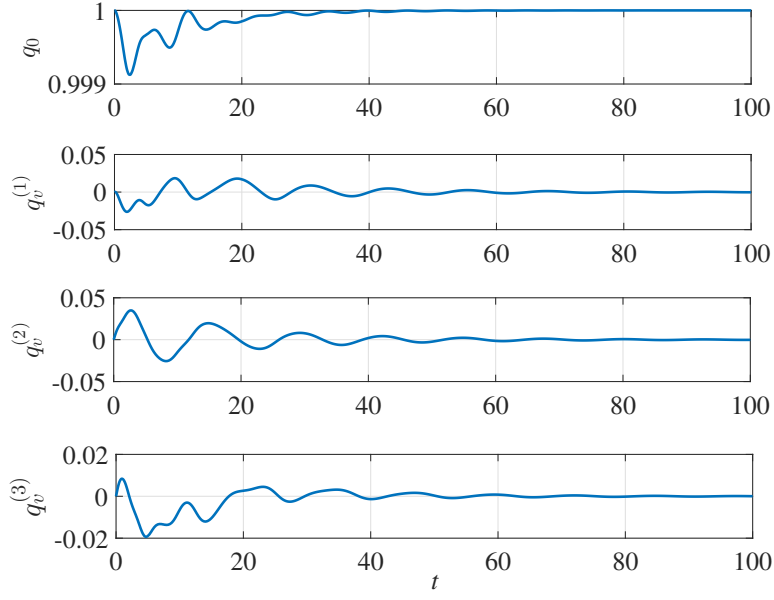


FIGURE 6. The time evolution of the quaternions; top subplot corresponds to q_0 and the remaining three correspond to the components of q_v .

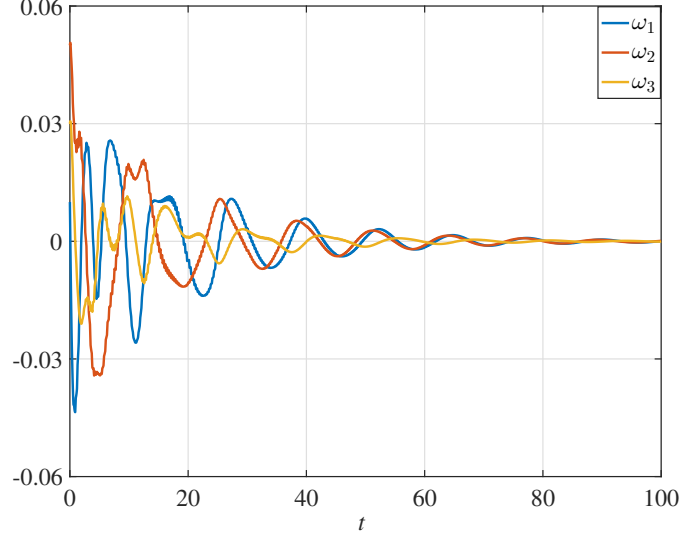


FIGURE 7. The time evolution of the angular velocities of the spacecraft.

of the equilibrium under slow switching. Fig. 10 also demonstrates that trajectories starting closer to the equilibrium take longer to exhibit divergence away from it. Thus, in order to stabilize the system one needs to reduce the switching time (equivalently, increase the switching frequency) appropriately as dictated by Theorem 2.4.

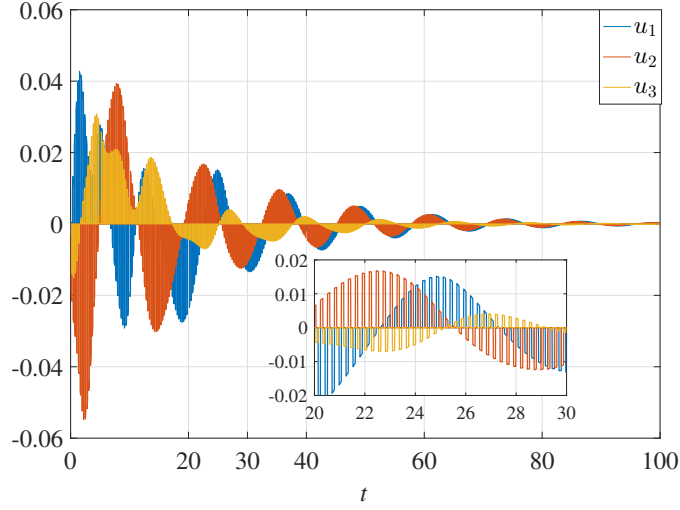


FIGURE 8. The control law implemented based on the periodic scheduling specified in §2.2. The zoomed in sub-plot clearly illustrates the round robin property of the controller.

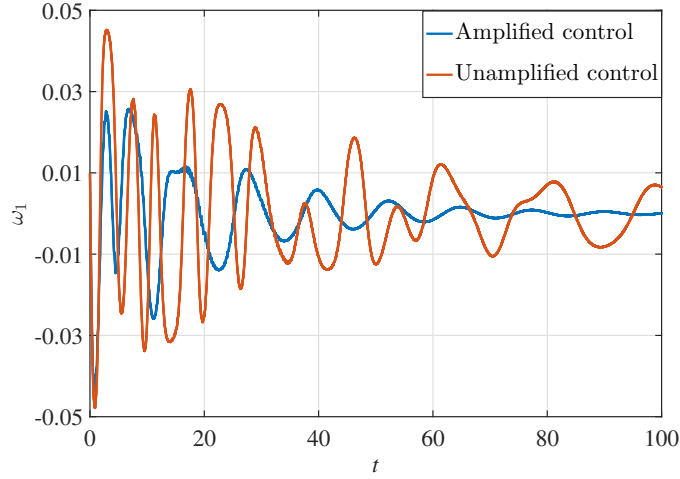


FIGURE 9. There is a significant qualitative improvement in performance when the control action is amplified. The trajectories plotted in the figure is that of ω_1 for both the amplified and the unamplified cases.

§4. CONCLUDING REMARKS AND FUTURE RESEARCH DIRECTIONS

We proposed two periodic scheduling schemes for a wide class of control-affine systems for which locally asymptotically stabilizing controllers are available, one leading to stability and the other to asymptotic stability. Numerical results were provided to illustrate the results.

A natural line of investigation is to quantify the performance of controllers and their convergence with respect to the frequency of the periodic scheduling. Moreover, it is of

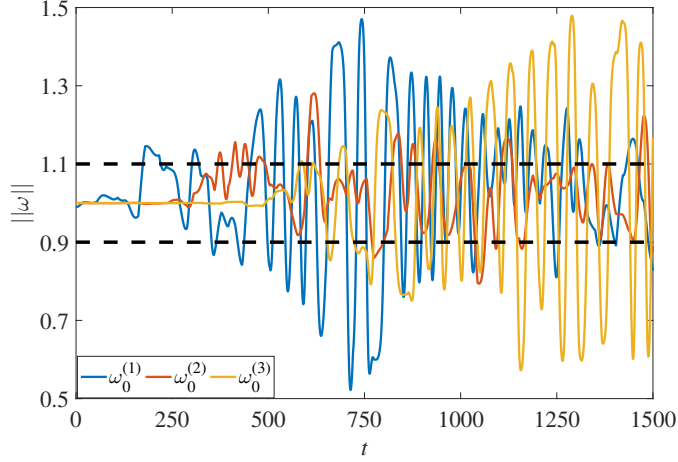


FIGURE 10. Round robin scheduling with a constant switching time of 18s. The trajectories of the spacecraft corresponding to $\|\omega\|$ digress away from the 0.1-ball around the equilibrium $x_e = (\bar{q}, 1, 0, 0)$ even if initialized very close to the equilibrium. $\omega_0^{(3)}$ is the initial condition closest to x_e among the three plotted here, and takes the longest to exhibit divergence.

significant interest to study the behavior of such systems under randomization as opposed to the round-robin scheduling treated herein. These topics will be taken up in subsequent works.

APPENDIX A. ESSENTIAL INGREDIENTS

This appendix collects some standard and not-so-standard results that are central to the proofs of Theorem 2.4 and Theorem 2.5 presented in §B.

§ A.1. Chattering lemma. We start with a version of the so-called “chattering lemma” [BM13, Theorem 3.6.1], which is popular in optimal control theory, applied to time-invariant right-hand sides.

Theorem A.1. *Let $n, q \in \mathbb{N}^*$, let $X \subset \mathbb{R}^n$ be a compact and nonempty set and let $I \subset \mathbb{R}$ be a compact interval. Define the maps $X \ni x \mapsto f_i(x) \in \mathbb{R}^n$, $i \in [q]$, satisfying the following properties:*

- (C-i) *each f_i is continuous in X ;*
- (C-ii) *there exist constants $L_1, L_2 > 0$ such that for all $x, y \in X$ and $i \in [q]$:*

$$\begin{aligned} \|f_i(x)\| &\leq L_1, \\ \|f_i(x) - f_i(y)\| &\leq L_2 \|x - y\|. \end{aligned}$$

Let $I \ni t \mapsto p^i(t) \in [0, +\infty]$, $i \in [q]$, be measurable maps satisfying

$$\sum_{i=1}^q p^i(t) = 1 \quad a.e.$$

Then for every $\bar{\varepsilon} > 0$ there exists a subdivision of \mathcal{I} into a finite collection $\{I_j\}_{j=1}^k$ of non-overlapping intervals and an assignment of one of the functions f_1, f_2, \dots, f_q to each I_j then for every t', t'' in \mathcal{I} and all $x \in \mathcal{X}$

$$(A.1) \quad \left\| \int_{t'}^{t''} \left(\sum_{i=1}^q p^i(t) f_i(x) - f_{\sigma(t)}(x) \right) dt \right\| < \bar{\varepsilon},$$

where the assignment is characterized by the map $\mathcal{I} \ni t \mapsto \sigma(t) \in [q]$.

We refer to the variable t as the *time* argument and the variable x as the *space* argument in the sequel.

Remark A.2. The candidate subdivision of the compact interval \mathcal{I} and an assignment of the functions f_i , for $i \in [q]$ into those subdivisions, whose existence is stated in Theorem A.1, as used in [BM13] is presented here. Define $\varepsilon := \frac{\bar{\varepsilon}}{2(2+|\mathcal{I}|)}$. For an integer \tilde{k} , we define a partition of \mathcal{I} into $\{\tilde{I}_j\}_{j \in [\tilde{k}]}$, such that $|\tilde{I}_j| < \frac{\varepsilon}{\max\{L_1, L_2\}}$. Further, for each j the interval \tilde{I}_j is subdivided into finitely many non-overlapping sub-intervals $E_{j,1}, E_{j,2}, \dots, E_{j,q}$ such that

$$|E_{j,i}| := \int_{I_j} p^i(t) dt \quad \text{for } i \in [q].$$

The assignment follows the rule

$$\sigma(t) = i \quad \text{for } t \in \text{int}(E_{j,i}), \quad i \in [q], \quad j \in [\tilde{k}].$$

We shall be employing this particular subdivision in the sequel.

§ A.2. Continuous dependence of solutions of a differential equation on parameters.

We state a result on the dependence of the solutions of a parameter-dependent differential equation on the parameter. For a positive scalar t_0 and some positive integers d and p , consider the two differential equations

$$(A.2) \quad \dot{\xi}(t) = F(t, \xi(t), \ell), \quad \xi(t_0) = \bar{x}, \quad t \geq t_0,$$

$$(A.3) \quad \dot{\zeta}(t) = F_*(t, \zeta(t)), \quad \zeta(t_0) = \bar{x}, \quad t \geq t_0,$$

where $\xi(t), \zeta(t) \in \mathbb{R}^d$ for each t , the (fixed) parameter ℓ takes values in \mathbb{R}^p , and the maps $[t_0, +\infty[\times \mathbb{R}^d \times \mathbb{R}^p \ni (t, x, \ell) \mapsto F(t, x, \ell) \in \mathbb{R}^d$ and $[t_0, +\infty[\times \mathbb{R}^d \ni (t, x) \mapsto F_*(t, x) \in \mathbb{R}^d$ satisfy the standard Carathéodory conditions [Fil88, Chapter 1]. We assume that both (A.2) and (A.3) have unique solutions and we denote these solutions by $[t_0, +\infty[\times \mathbb{R}^p \ni (t, \ell) \mapsto \xi(t, \ell) \in \mathbb{R}^d$ for (A.2) and by $[t_0, +\infty[\ni t \mapsto \zeta(t) \in \mathbb{R}^d$ for (A.3), where we suppress the dependence of solution trajectories on both the initial time instant t_0 and the initial condition \bar{x} for the sake of brevity. The following theorem provides a set of sufficient conditions for the convergence of the trajectories of (A.2) to those of (A.3) on a compact interval.

Theorem A.3. [Fil88, Chapter 1, Theorem 7] *Consider the differential equations (A.2) and (A.3). Define a compact interval $\mathcal{I} := [t_0, t_1]$ for some scalars $t_0 < t_1$ and a compact set $\mathcal{K} \subset \mathbb{R}^d$ containing the point \bar{x} . Let*

- (A-i) *the function $F(t, x, \ell)$ be measurable in t for constant x, ℓ ; and the function $F_*(t, x)$ be measurable in t for constant x ;*
- (A-ii) *$\|F(t, x, \ell)\| \leq m(t, \ell)$, where $\mathbb{R} \times \mathbb{R}^p \ni (t, \ell) \mapsto m(t, \ell) \in \mathbb{R}$ is summable in t ; similarly $\|F_*(t, x)\| \leq m_*(t)$, where $\mathbb{R} \ni t \mapsto m(t, \ell) \in \mathbb{R}$ is summable in t ;*

(A-iii) there exists a summable function $\mathcal{I} \in t \mapsto l(t) \in \mathbb{R}$ and a monotone function $\mathbb{R}^d \ni x \mapsto \psi(x) \in \mathbb{R}$ satisfying $\psi(x) \rightarrow 0$ as $x \rightarrow 0$, such that for each $r > 0$, for all $x, y \in \mathcal{K}$ satisfying $\|x - y\| \leq r$ and for almost all $t \in \mathcal{I}$ we have

$$(A.4) \quad \begin{aligned} \|F(t, x, \ell) - F(t, y, \ell)\| &\leq l(t)\psi(r) \text{ and} \\ \|F_*(t, x) - F_*(t, y)\| &\leq l(t)\psi(r); \end{aligned}$$

(A-iv) for each $x \in \mathcal{K}$ and any sequence $\ell_i \xrightarrow{i \rightarrow +\infty} \ell_*$, we have

$$(A.5) \quad \int_{t_0}^t F(s, x, \ell) \, ds \xrightarrow{i \rightarrow +\infty} \int_{t_0}^t F_*(s, x) \, ds$$

uniformly in t on the interval \mathcal{I} .

Then for every $\varepsilon > 0$ there exists a scalar $\eta > 0$ such that for all ℓ satisfying $\|\ell - \ell_*\| < \eta$, each solution $\xi(\cdot, \ell)$ of (A.2) (corresponding to the initial condition $\bar{x} \in \mathcal{K}$) exists on the interval $[t_0, t_1]$ and satisfies

$$\|\xi(t, \ell) - \zeta(t)\| < \varepsilon \quad \text{for } t \in [t_0, t_1] \text{ and } \|\ell - \ell_*\| < \eta.$$

§A.3. A version of Alekseev's bound. At this juncture we state a result from [TB19] that provides a bound on the difference between solution trajectories of a class of autonomous differential equations when initialized at two different initial conditions. For a positive integer d and a scalar t_0 , consider the following differential equation

$$(A.6) \quad \dot{x}(t) = h(x(t)), \quad x(t_0) = \bar{x}, \quad t \geq t_0,$$

where the map $\mathbb{R}^d \ni x \mapsto h(x) \in \mathbb{R}^d$ is continuously differentiable. We denote the solution of (A.6) by $t \mapsto x(t, t_0, \bar{x})$ for $t \geq t_0$. Let $0 \in \mathbb{R}^d$ be an *isolated, hyperbolic and locally asymptotically stable* equilibrium of (A.6) and let \mathcal{K} be a bounded set containing 0 in its interior and that is contained in the domain of attraction of the equilibrium point 0.

Recall that a continuously differentiable function $V : \text{dom}(V) \subset \mathbb{R}^d \rightarrow \mathbb{R}$ is said to be a *Lyapunov function* for the equilibrium point 0 if $\text{dom}(V)$ is open, $V(0) = 0$, and for all $x \neq 0$, the estimates $V(x) > 0$ and $\langle \nabla V(x), h(x) \rangle < 0$ hold simultaneously. The converse Lyapunov Theorem [Vid02, Chapter 5] guarantees the existence of a Lyapunov function near a locally asymptotically stable equilibrium point 0. In fact, we can choose V so that $V(x) \rightarrow +\infty$ as x tends to the boundary of the $\text{dom}(V)$. Let V be a Lyapunov function for (A.6) such that $\text{dom}(V)$ denotes the domain of the Lyapunov function V . For $p > 0$ we define $V^{(p)} := V^{-1}(p)$, and for $q > 0$ we let

$$\mathcal{N}_q(V^{(p)}) := \bigcup_{y \in V^{(p)}} \mathcal{B}[y, q].$$

From elementary properties of Lyapunov functions we see that there exist scalars r, r_0, ε_0 such that $r > r_0$ and for each $\varepsilon \in]0, \varepsilon_0[$ we have

$$(A.7) \quad \mathcal{B}[0, \varepsilon] \subset \mathcal{K} \subset V^{(r_0)} \subset \mathcal{N}_{\varepsilon_0}(V^{(r_0)}) \subset V^{(r)} \subset \text{dom}(V).$$

A pictorial representation of the above statement is presented in Fig. 11.

Let $Dh(0)$ be the Jacobian matrix of h evaluated at 0. Since the equilibrium point 0 is hyperbolic and locally asymptotically stable, the matrix $Dh(0)$ is guaranteed to be Hurwitz.³

³The assumption of the equilibrium point being 0 is missing from [TB19].

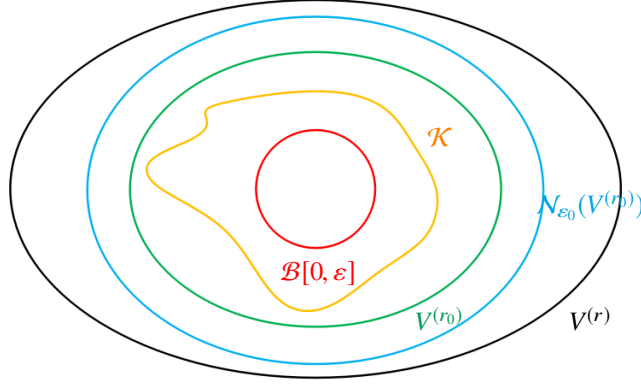


FIGURE 11. Pictorial depiction of the sets in (A.7).

Let $\lambda_1, \lambda_2, \dots, \lambda_d$, with possible repetitions, denote the eigenvalues of the matrix $Dh(0)$. We define

$$\lambda_{\min} := \min_{i \in [d]} \{ -\Re(\lambda_i) \}.$$

Fix two scalars $\lambda', \kappa > 0$ such that $\lambda' < \lambda_{\min}$ and $0 < \kappa < 1$. Then [Tes12, Corollary 3.6] asserts that there exists a constant $\tilde{K} > 0$ such that

$$\|e^{Dh(0)t}\| \leq \tilde{K}e^{-\lambda't} \text{ for all } t \geq 0.$$

Theorem A.4. [TB19, Lemma 5.1] *Consider the system (A.6) along with its associated data and adopt the notations developed above. Define*

$$(A.8) \quad \lambda := \frac{1-\kappa}{\tilde{K}^2} \lambda'.$$

Let r be chosen as stated in (A.7), let u_1, u_2 be arbitrary points in $V^{(r)}$, and let $s \geq 0$. Then

$$\|x(t, s, u_1) - x(t, s, u_2)\| \leq K_1 \|u_1 - u_2\| e^{-\lambda(t-s)} \text{ for all } t \geq s,$$

where K_1 is a constant that depends on the set \mathcal{K} and the vector field h .

APPENDIX B. PROOFS OF THE MAIN RESULTS

For a consistent notation throughout the rest of this section, we shall denote the trajectories of (2.3) by $x(\cdot)$, of (2.5) by $y(\cdot)$, and of (2.7) by $z(\cdot)$.

§B.1. Proof of Theorem 2.4. The proof unfolds in the following two key steps:

- (M-i) We bound the difference between trajectories of (2.3) and (2.5) on a compact time interval. To accomplish this, we appeal to Theorem A.3;
- (M-ii) We iteratively extend the preceding bound over the entire time horizon $[t_0, +\infty[$ by repeatedly invoking Theorem A.3 in conjunction with Theorem A.4. Local asymptotic stability of the equilibrium $0 \in \mathbb{R}^d$ of the closed-loop system (2.3) plays a crucial role in the arguments of the proof.

We proceed to the comprehensive proof of Theorem 2.4.

• **Step-I:** As the equilibrium $0 \in \mathbb{R}^d$ of (2.3) is asymptotically stable, we can find a $c > 0$ such that if $\|\bar{x}\| \leq c$ then $\|x(t)\| \xrightarrow[t \rightarrow +\infty]{} 0$. Fix $\nu > 0$, and define $\beta := \min(\nu, c)$. Define a compact set $\mathcal{K} := \mathcal{B}[0, \beta]$. Pick a scalar $\alpha \in]0, 1[$ and define the another compact set $\mathcal{K}_\alpha := \mathcal{B}[0, \alpha\beta]$. Also, the equilibrium point $0 \in \mathbb{R}^d$ of (2.3) is stable in the sense of Lyapunov therefore we can find a positive scalar Δ such that if $\|\bar{x}\| \leq \Delta$ then $x(t) \in \mathcal{K}_\alpha$ for all $t \geq t_0$. In other words, the trajectory $x(\cdot) \subset \mathcal{K}_\alpha \subset \mathcal{K}$.

For $T > 0$, define $\Theta := K_1 e^{-\lambda T}$, where K_1, λ are positive scalars which depend on the set \mathcal{K} and the closed-loop vector field governing (2.3). Choose the scalar T such that $\Theta < 1$. We partition the interval $[t_0, +\infty[$ into a countable family of disjoint half-open intervals of length T as $[t_0, +\infty[= \bigcup_{n \in \mathbb{N}} I_n$ where $I_n := [t_0 + nT, t_0 + (n+1)T[$. We now provide a uniform bound on the difference between the trajectories of (2.3) and (2.5) over a compact interval by appealing to Theorem A.3.

The requirements of Theorem A.3 except (A-iv) are trivially met by the right hand sides of (2.3) and (2.5) since these are the standard Carathéodory conditions. We claim that (A-iv) is also satisfied in view of Theorem A.1 and Remark A.2. To verify this we define the map

$$\mathbb{R}^d \ni x \mapsto H_i(x) := f(x) + mg_i(x)\phi_i(x) \in \mathbb{R}^d,$$

a partition of unity as $[t_0, +\infty[\ni t \mapsto p^i(t) = \frac{1}{m} \in [0, +\infty[$ for each $i \in [m]$, and the time-varying map

$$[t_0, +\infty[\times \mathbb{R}^d \times]0, +\infty[\ni (t, x, \tilde{\tau}) \mapsto F(t, x, \tilde{\tau}) := H_{\sigma(t-t_0, \tilde{\tau})}(x) \in \mathbb{R}^d,$$

where $\sigma(\cdot)$ is as defined in (2.4). These definitions permit us to write (2.3) as

$$\dot{x}(t) = \sum_{i=1}^m p^i(t) H_i(x(t)), \quad x(t_0) = \bar{x}, \quad t \geq t_0,$$

and (2.5) as

$$\dot{y}(t) = F(t, y(t), \tau), \quad y(t_0) = \bar{x}, \quad t \geq t_0.$$

Moreover, from Theorem A.1 for $t \in I_k$ ($k \in \mathbb{N}$) and all $z \in \mathcal{K}$ we have

$$(B.1) \quad \int_{t_0+kT}^t \left(\sum_{i=1}^m p^i(s) H_i(z) - F(s, z, \tau) \right) ds \xrightarrow[\tau \downarrow 0]{} 0 \quad \text{uniformly in } t,$$

which confirms the claim.

Against the preceding backdrop, it is immediate from Theorem A.3 that the trajectory $y(\cdot)$ converges uniformly to $x(\cdot)$ on the interval I_0 . That is, for each $\gamma > 0$ there exists a switching time $\bar{\tau}$ sufficiently small such that

$$(B.2) \quad \sup_{t \in I_0} \|x(t) - y(t)\| \leq \gamma.$$

At this stage pick $\gamma < \frac{\beta(1-\alpha)}{K_2}$ with $K_2 := 1 + \frac{K_1}{1-\Theta}$, and corresponding to this value of γ we select $\bar{\tau}$ such that (B.2) is satisfied, and keep this $\bar{\tau}$ fixed through the end of the current proof.

For the next step of the proof we shall retain the notation of $y(\cdot)$ for the solution trajectory of (2.5) but we emphasize that this trajectory corresponds to the switching time $\bar{\tau}$ fixed above.

• **Step-II:** In order to extend the uniform bound in (B.2) to $[t_0, +\infty[= \bigcup_{k \in \mathbb{N}^*} I_k$, we appeal to the results of Theorem A.3 over successive intervals I_k . Note that it was possible to use the results of Theorem A.3 to uniformly bound the separation between two trajectories $x(\cdot)$ and $y(\cdot)$ over I_0 because the two trajectories start from the same state at time t_0 (along with other requirements posited in Theorem A.3). However, once the system has evolved over time interval I_0 , the two trajectories $x(\cdot)$ and $y(\cdot)$ may not necessarily intersect at any future time, and thus there is no direct way to use Theorem A.3. To circumvent this problem, we construct an ensemble of trajectories $(x_{(n)}(\cdot))_{n \in \mathbb{N}^*}$, each of which satisfies the dynamics given in (2.3) with the initial conditions,

$$(B.3) \quad x_{(n)}(t_0 + nT) = y(t_0 + nT) \quad \text{for each } n \in \mathbb{N}^*.$$

That is, for $t \in I_k$, the differential equation governing $x_{(k)}(\cdot)$ is

$$\dot{x}_{(k)}(t) = \sum_{i=1}^m p^i(t) H_i(x_{(k)}(t)), \quad x_{(k)}(t_0 + kT) = y(t_0 + kT), \quad t \in I_k.$$

Employing the fact that the vector fields H_i are time-invariant along with the vector field F being invariant under time shift by $m\bar{\tau}$ and (B.3), we can conclude from Theorem A.3 that

$$(B.4) \quad \sup_{t \in I_k} \|x_{(k)}(t) - y(t)\| \leq \gamma \quad \text{for each } k \in \mathbb{N}^*,$$

where the switching time is chosen to be $\bar{\tau}$, which is identical to the one selected in (B.2).

We claim that the difference between $y(\cdot)$ and $x(\cdot)$ at $t = t_0 + nT$ for every $n \in \mathbb{N}^*$ satisfies the estimate

$$(B.5) \quad \|y(t_0 + nT) - x(t_0 + nT)\| \leq \gamma \left(\sum_{i=0}^{n-1} K_1^i e^{-i\lambda T} \right).$$

The preceding claim is established inductively. For the induction base, consider $n = 2$. At $t = t_0 + 2T$, we have

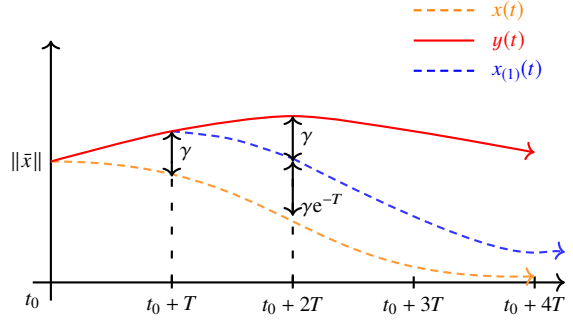
$$\begin{aligned} \|y(t_0 + 2T) - x(t_0 + 2T)\| &\leq \|y(t_0 + 2T) - x_{(1)}(t_0 + 2T)\| + \|x_{(1)}(t_0 + 2T) - x(t_0 + 2T)\| \\ &\leq \gamma + K_1 \gamma e^{-\lambda T} \quad \text{in view of (B.4) and Theorem A.4.} \end{aligned}$$

Fix $q \in \mathbb{N}^*$, and assume, as the induction hypothesis, that the claim holds for each $n \in [q-1]$. Define $t_q := t_0 + qT$. For the induction step $n = q$, we observe that

$$\begin{aligned} \|y(t_q) - x(t_q)\| &\leq \|y(t_q) - x_{(q-1)}(t_q)\| + \|x_{(q-1)}(t_q) - x(t_q)\| \\ &\leq \gamma + K_1 \left(\gamma \left(\sum_{i=0}^{q-2} K_1^i e^{-i\lambda T} \right) e^{-\lambda T} \right) \quad \text{in view of (B.5),} \end{aligned}$$

which proves the claim (B.5). A pictorial depiction of the bounding process (B.5) is provided in Fig. 12. Note that the right hand side of (B.5) is valid for time instants that are integral multiples of T starting at t_0 . The corresponding bound for a general time $t \in [t_0, +\infty[$ is given by

$$(B.6) \quad \|y(t) - x(t)\| \leq \gamma + K_1 \left(\gamma \left(\sum_{i=0}^{\hat{t}-1} K_1^i e^{-i\lambda T} \right) \right),$$

FIGURE 12. Norm of solutions vs time for the case when $K_1 = 1$

where $\hat{t} := \left\lfloor \frac{t-t_0}{T} \right\rfloor$ for $t \geq t_0 + T$, where we have employed (B.5) to arrive at (B.6). Indeed, for $t \in]t_0 + \hat{t}T, t_0 + (\hat{t} + 1)T[$ we have

$$\begin{aligned} \|y(t) - x(t)\| &\leq \|y(t) - x_{(\hat{t})}(t)\| + \|x_{(\hat{t})}(t) - x(t)\| \\ &\leq \gamma + K_1 \left(\gamma \left(\sum_{i=0}^{\hat{t}-1} K_1^i e^{-i\lambda T} \right) e^{-\lambda(t-\hat{t}T)} \right) \quad \text{in view of (B.5) and Theorem A.4} \\ &\leq \gamma + K_1 \left(\gamma \left(\sum_{i=0}^{\hat{t}-1} K_1^i e^{-i\lambda T} \right) \right). \end{aligned}$$

Based on the selection criterion of T , we have $\Theta < 1$; thus, we can bound the expression in (B.6) by the sum of the geometric series, leading to

$$\| \|y(t)\| - \|x(t)\| \| \leq \|y(t) - x(t)\| \leq \gamma \left(1 + \frac{K_1}{1 - \Theta} \right) \quad \text{for all } t \geq t_0.$$

As a consequence, we arrive at

$$(B.7) \quad \|y(t)\| \leq \|x(t)\| + K_2 \gamma \leq \nu \quad \text{for all } t \geq t_0,$$

where the last inequality is due to the choice of γ made earlier.

This concludes the proof of Theorem 2.4 since for every $\nu > 0$ we have exhibited a $\Delta > 0$ and a switching time $\bar{\tau} > 0$ (refer to **Step-I**), both of which are independent of the initial time t_0 and depend only on ν , such that

$$\|y(t)\| \leq \nu \quad \text{for } t \geq t_0 \text{ if } \|\bar{x}\| \leq \Delta.$$

§ B.2. Proof of Theorem 2.5. This proof follows the same steps as that of Theorem 2.4, namely (M-i)-(M-ii).

As the equilibrium $0 \in \mathbb{R}^d$ of (2.3) is asymptotically stable, we can find a $c > 0$ such that if $\|\bar{x}\| \leq c$ then $\|x(t)\| \xrightarrow[t \rightarrow +\infty]{} 0$. Fix $\nu > 0$, and define $\beta := \min(\nu, c)$. Define a compact set $\mathcal{K} := \mathcal{B}[0, \beta]$. Pick a scalar $\alpha \in]0, 1[$ and define the another compact set $\mathcal{K}_\alpha := \mathcal{B}[0, \alpha\beta]$. Also, the equilibrium point $0 \in \mathbb{R}^d$ of (2.3) is stable in the sense of Lyapunov therefore we can find a positive scalar Δ such that if $\|\bar{x}\| \leq \Delta$ then $x(t) \in \mathcal{K}_\alpha$ for all $t \geq t_0$. In other words, the trajectory $x(\cdot) \subset \mathcal{K}_\alpha \subset \mathcal{K}$.

Pick $\eta \in]0, 1[$. For $T > 0$, define $\Theta := \frac{K_1}{\eta} e^{-\lambda T}$, where K_1, λ are positive scalars which depend on the set \mathcal{K} and the closed-loop vector field governing (2.3). Choose $T > 0$ such that $\Theta < 1$. As in §B.1, we partition the interval $[t_0, +\infty[$ into a countable family of disjoint half-open intervals of length T as $[t_0, +\infty[= \bigcup_{n \in \mathbb{N}} I_n$ where $I_n := [t_0 + nT, t_0 + (n+1)T[$.

As in the proof of Theorem 2.4, we appeal to Theorem A.3 to claim that the trajectory $z(\cdot)$ converges uniformly to $x(\cdot)$ on the interval I_0 . That is, for any $\gamma > 0$ there exists a switching time τ sufficiently small such that

$$(B.8) \quad \|z(t) - x(t)\| \leq \gamma \quad \text{for } t \in I_0.$$

At this stage pick $\gamma < \frac{\beta(1-\alpha)}{K_2}$ with $K_2 := 1 + \frac{K_1}{1-\Theta}$, and corresponding to this value of γ we select $\bar{\tau}$ such that (B.8) is satisfied. For $t \in I_0$, we set $\tilde{\tau}(t) = \bar{\tau}$.

Analogous to the proof of Theorem 2.4, we construct an ensemble of trajectories $(\tilde{x}_{(k)}(\cdot))_{k \in \mathbb{N}^*}$ each satisfying the dynamics (2.7), and the condition that

$$\tilde{x}_{(n)}(t_0 + nT) = z(t_0 + nT), \quad \text{for all } n \in \mathbb{N}^*.$$

For each of the time intervals I_i ($i \in \mathbb{N}^*$), we choose a switching time $\tau_i \in \mathbb{R}$ such that

$$\|z(t) - \tilde{x}_{(i)}(t)\| \leq \eta^i \gamma \quad \text{for } t \in I_i,$$

where a priori. Note that the existence of such τ_i is guaranteed by Theorem A.3. In fact, it is possible to pick $\tau_i \geq \tau_{i+1}$ for all $i \in \mathbb{N}^*$. We set $\tilde{\tau}(t) = \tau_i$ for $t \in I_i$ and $i \in \mathbb{N}^*$.

We claim that the difference between $z(\cdot)$ and $x(\cdot)$, at each time t , satisfies the estimate

$$(B.9) \quad \|z(t) - x(t)\| \leq \eta^{\hat{t}} \gamma + K_1 \left(\gamma \left(\sum_{i=0}^{\hat{t}-1} \eta^{\hat{t}-1-i} K_1^i e^{-i\lambda T} \right) \right),$$

where $\hat{t} = \left\lfloor \frac{t-t_0}{T} \right\rfloor$ for $t \geq t_0 + T$. Proof of which is exactly on the lines of the proof of (B.6) in §B.1.

Based on the selection criterion of T , we have $\Theta < 1$ and therefore we can bound (B.9) as follows:

$$(B.10) \quad \left| \|z(t)\| - \|x(t)\| \right| \leq \|z(t) - x(t)\| \leq \eta^{\hat{t}} \gamma \left(1 + \frac{K_1}{1-\Theta} \right) \quad \text{for } t \geq t_0.$$

The above inequality suggests that

$$(B.11) \quad \|z(t)\| \leq \|x(t)\| + \eta^{\hat{t}} K_2 \gamma \quad \text{for } t \geq t_0.$$

Since the equilibrium of (2.3) is locally asymptotically stable there exists Δ' such that for every $\psi > 0$ there exists $T' > 0$ such that

$$\|\bar{x}\| \leq \Delta' \implies \|x(t)\| \leq \frac{\psi}{2} \quad \text{for all } t \geq t_0 + T'.$$

Using (B.11) and setting $\|\bar{x}\| \leq \min(\Delta, \Delta')$ we can conclusively say that for every $\psi > 0$ if we define

$$(B.12) \quad T_{AS} := \max \left(T', \frac{\log(\frac{\psi}{2K_2\gamma})}{\log(\eta)} \right),$$

which is independent of t_0 , then $\|z(t)\| \leq \psi$ for all $t \geq t_0 + T_{AS}$. Our proof is complete.

Remark B.1. It is evident from (B.12) that the time required for the trajectories $z(\cdot)$ to reach any neighborhood of the equilibrium point 0 is at least as large as that for the trajectories $x(\cdot)$. This observation is quite natural since a loss of performance is expected due to the round-robin periodic scheduling of control channels.

REFERENCES

- [Art08] Z. Artstein. A Young measures approach to averaging. In *Differential Equations, Chaos and Variational Problems*, volume 75 of *Progress in Nonlinear Differential Equations and their Applications*, pages 15–28. Birkhäuser, Basel, 2008.
- [BM13] L. D. Berkovitz and N. G. Medhin. *Nonlinear Optimal Control Theory*. Chapman & Hall/CRC Applied Mathematics and Nonlinear Science Series. CRC Press, Boca Raton, FL, 2013.
- [CC10] B. Chen and H. Cheng. A review of the applications of agent technology in traffic and transportation systems. *IEEE Transactions on Intelligent Transportation Systems*, 11(2):485–497, 2010.
- [CHW11] R. Claes, T. Holvoet, and D. Weyns. A decentralized approach for anticipatory vehicle routing using delegate multi agent systems. *IEEE Transactions on Intelligent Transportation Systems*, 12(2):364–373, 2011.
- [CM12] A. Chakraborty and D. Marija, editors. *Control and Optimization Methods for Electric Smart Grids*. Power Electronics and Power Systems. Springer, New York, 2012.
- [CPRT17] M. Caponigro, B. Piccoli, F. Rossi, and E. Trélat. Sparse Jurdjevic-Quinn stabilization of dissipative systems. *Automatica*, 86:110–120, 2017.
- [Fil88] A. F. Filippov. *Differential Equations with Discontinuous Righthand Sides*, volume 18 of *Mathematics and its Applications (Soviet Series)*. Kluwer Academic Publishers Group, Dordrecht, 1988. Translated from the Russian.
- [GB08] F. E. Guezar and H. Bouzahir. Chaotic behavior in a switched dynamical system. *Modelling and Simulation in Engineering*, 2008:2, 2008.
- [GIL07] D. Görges, M. Izák, and D. Liu. Optimal control of systems with resource constraints. In *Proceedings of the 46th IEEE Conference on Decision and Control*, pages 1070–1075, 2007.
- [JQ78] V. Jurdjevic and J. P. Quinn. Controllability and stability. *Journal of Differential Equations*, 28(3):381–389, 1978.
- [KC17] A. Kundu and D. Chatterjee. Stabilizing switching signals: a transition from point-wise to asymptotic conditions. *Systems & Control Letters*, 106:16–23, 2017.
- [LA05] M. Lovera and A. Astolfi. Global magnetic attitude control of inertially pointing spacecraft. *Journal of Guidance, Control, and Dynamics*, 28(5):1065–1072, 2005.
- [Lib03] D. Liberzon. *Switching in Systems and Control*. Systems & Control: Foundations & Applications. Birkhäuser Boston, Inc., Boston, MA, 2003.
- [MSBH17] A. V. Maas, Y. F. Steinbuch, A. Boverhof, and W. P. Heemels. Switched control of a SCARA robot with shared actuation resources. *IFAC-PapersOnLine*, 50(1):1931–1936, 2017.
- [PKS13] B. Polyak, M. Khlebnikov, and P. Shcherbakov. An LMI approach to structured sparse feedback design in linear control systems. In *Proceedings of the European Control Conference*, pages 833–838, 2013.
- [PL01] E. Panteley and A. Loría. Uniform exponential stability for parameterized linear “skew-symmetric” systems. In *Proceedings of European Control Conference*, pages 2410–2415. IEEE, 2001.
- [SA11] S. Sukumar and M. R. Akella. Precision attitude stabilization: Incorporating rise and fall times in gas-based thrusters. *Journal of Guidance, Control, and Dynamics*, 34(1):317–323, 2011.
- [TB19] G. Thoppe and V. Borkar. A concentration bound for stochastic approximation via Alekseev’s formula. *Stochastic Systems*, 9(1):1–26, 2019.
- [Tes12] G. Teschl. *Ordinary Differential Equations and Dynamical Systems*, volume 140. American Mathematical Society, 2012.
- [Vid02] M. Vidyasagar. *Nonlinear Systems Analysis*. Classics in Applied Mathematics. SIAM, 2nd edition, 2002.
- [WD91] J. T. Wen and K. K. Delgado. The attitude control problem. *IEEE Transactions on Automatic control*, 36(10):1148–1162, 1991.
- [WY01] G. C. Walsh and H. Ye. Scheduling of networked control systems. *IEEE Control Systems Magazine*, 21(1):57–65, 2001.